Biocompatible and detectable carboxylated nanodiamond on human cell



2007 Nanotechnology 18 325102

(http://iopscience.iop.org/0957-4484/18/32/325102)

Nanotechnology **18** (2007) 325102 (10pp) doi:10.1088/0957-4484/18/32/325102

# Biocompatible and detectable carboxylated nanodiamond on human cell

**Kuang-Kai Liu**[1,2], **Chia-Liang Cheng**[3], **Chia-Ching Chang**[4,5,6] **and Jui-I Chao**[1,2,7]

[1] Institute of Pharmacology and Toxicology, Tzu Chi University, Hualien 970, Taiwan
[2] Biomedical Nanotechnology Laboratory, Tzu Chi University, Hualien 970, Taiwan
[3] Department of Physics, National Dong Hwa University, Hualien 974, Taiwan
[4] Department of Biological Science and Technology, National Chiao Tung University, Hsin-Chu 300, Taiwan
[5] Institute of Physics, Academia Sinica, Taipei 11529, Taiwan
[6] National Nano Device Laboratories, Hsinchu 30078, Taiwan

E-mail: chaoji@mail.tcu.edu.tw

Received 24 May 2007
Published 13 July 2007
Online at stacks.iop.org/Nano/18/325102

**Abstract**

Surface-modified carboxylated nanometre-sized diamond (cND) has been applied for the conjugation of biological molecules such as DNA and protein. In this study, we evaluated the biocompatibility and detection of cNDs and carbon nanotubes on human lung A549 epithelial cells and HFL-1 normal fibroblasts. Treatment with 5 or 100 nm cND particles, 0.1–100 $\mu$g ml$^{-1}$, did not reduce the cell viability and alter the protein expression profile in lung cells; however, carbon nanotubes induced cytotoxicity in these cells. The cNDs particles were accumulated in A549 cells, which were observed by atomic force microscopy and laser scanning confocal microscopy. Both 5 and 100 nm cNDs particles exhibited the green fluorescence and were ingested into cells. Moreover, the fluorescence intensities were increased in cells via a concentration-dependent manner after treatment with 5 and 100 nm cNDs, which can be detected by flow cytometer analysis. The fluorescence intensities of 5 nm cNDs were relative higher than 100 nm cNDs in cells at equal concentration treatment. The observation demonstrated that cND-interacting with cell is detectable by a confocal microscope, flow cytometer and atomic force microscope. These nanoparticles may be useful for further biomedical applications based on the properties of uptake ability, detectability and little cytotoxicity in human cells.

(Some figures in this article are in colour only in the electronic version)

## 1. Introduction

Carbon derivative nanoparticles including carbon nanotubes, carbon nanofibres, fullerenes ($C_{60}$) and nanodiamonds, have been evaluated for bio-application because of their excellent electronic and chemical properties [1–3]. The nanodiamond surfaces provide a unique platform for bio-conjugation after chemical modifications [2, 3]. Modification on the surface of nanodiamond by carboxylation (carboxylated nanodiamond, cND) exhibits high affinity for proteins [4]. It has been reported that the modified surface of nanodiamonds can be conjugated with bio-molecules such as DNA [3, 5], cytochrome c [6] and antigen [7].

Development of nanoparticles conjugated with biological molecules for biomedical application has been intensively investigated in recent years [8, 9]. The advanced techniques of imaging and manipulation *in vivo* with nanoprobes such

[7] Address for correspondence: Institute of Pharmacology and Toxicology, College of Life Sciences, Tzu Chi University, 701, Section 3, Chung-Yang Road, Hualien 970, Taiwan.

 

as quantum dots (qdots) [10, 11] and gold nanoparticles [12] have been studied in several reports. Nanoparticles are potentially used as novel probes for both diagnostic and therapeutic applications [8, 9, 11]. A variety of particle sizes and compositions of qdots display different fluorescence colours that are stable and suitable for bio-labelling and -detection [8]. For example, the ZnS-capped CdSe qdots coated with a lung-targeting peptide can be accumulated in the lungs of mice after vascular injection [8]. Moreover, the specific peptide- or antibody-conjugated qdots can target tumours of mice [8, 13]. However, the existence of heavy metals in qdots such as cadmium, a well-established human toxicant and carcinogen, poses potential danger for further medical application. As the use of nanomaterials for biomedical applications is increasing, environmental pollution and toxicity have to be addressed. Unfortunately, few studies have investigated the toxicological and environmental effects of direct and indirect exposure to nanomaterials [14]. Determination of the potential human health effects from exposure to nanoparticles can be established by toxicity tests including *in vitro* (cellular and non-cellular) and *in vivo* (animal) assays [15, 16]. Recently, carbon nanomaterials showed quite different cytotoxicity [17]. The cytotoxic sequence order was found to be nanotubes > quartz > $C_{60}$ toward alveolar macrophage [17]. Accordingly, the development of a non-toxic and biocompatible nanomaterial is required.

In the present study, various sizes of cNDs were evaluated on the cytotoxicity in human lung cells. The 5 and 100 nm cND particles were accumulated on A549 lung epithelial cells and HFL-1 lung fibroblast; however, these cND particles did not induce cytotoxicity and apoptosis. Interestingly, both 5 and 100 nm cNDs display natural green fluorescence upon laser excitation in cells that can be detected by scanning confocal microscopy and flow cytometry. Recently, high energy treated nanodiamond was found to emit bright fluorescence and no photobleaching was detected [18]. The biocompatible and detectable properties of cND nanoparticles are considered as a novel and relative safe nanomaterial for further biomedical applications.

## 2. Experimental details

### 2.1. Chemicals and reagents

The powder of nanodiamonds (NDs) with an average 5 nm diameter was from Toron (ultrFine Diamond, Russia). The 100 nm ND powder was from General Electric Company (GE, USA). The powders of 10–50 nm and 100–200 nm carbon nanotubes (CNTs) were from Yonyu Applied Technology Material Corporation (Tainan, Taiwan). Hoechst 33258, 3-(4,5-dimethyl-thiazol-2-yl) 2,5-diphenyl tetrazolium bromide (MTT), sodium arsenite ($NaAsO_2$), and the Cy3-labeled mouse anti-$\beta$-tubulin (c-4585) were purchased from Sigma Chemical Co. (St Louis, MO).

### 2.2. Preparation of cNDs and cCNTs

The standard procedure for cNDs preparation was used according to the previous study with some modification [6]. Briefly, 0.2 g powder of NDs or CNTs were added into 15 ml acid mixture of $H_2SO_4$:$HNO_3$ (3:1) in an ultrasonic bath for 24 h, then in 0.1 M NaOH aqueous solution at 90 °C for 2 h, finally in 0.1 M HCl aqueous solution at 90 °C for 2 h. Thereafter, the treated nanodiamonds were washed with distilled water and then subjected to high speed centrifugation for several times to collect the sediment and dry. After drying, these particles were dissolved in distilled water. The solution of cNDs or carboxylated CNTs (cCNTs) will be sonicated for 20 min before treatment with cells.

### 2.3. Cell culture

The A549 lung epithelial cell line (ATCC number: CCL-185) was derived from the lung adenocarcinoma of a 58 year old Caucasian male. HFL-1 (ATCC number: CCL-153) is normal lung fibroblast that was derived from a Caucasian fetus. A549 cells were maintained in RPMI-1640 medium (Invitrogen Co., Carlsbad, CA). HFL-1 cells were cultured in DMEM medium (Invitrogen). The complete media were supplemented with 10% foetal bovine serum. These cells were cultured at 37 °C and 5% $CO_2$ in a humidified incubator (310/Thermo, Forma Scientific, Inc., Marietta, OH).

### 2.4. Cytotoxicity assay

The cells were plated in 96-well plates at a density of $1 \times 10^4$ cells/well for 16–20 h. Then the cells were treated with 0–100 $\mu$g ml$^{-1}$ nanoparticles in complete medium. After treatment, the cells were washed twice with phosphate-buffered saline (PBS), and were re-cultured in complete medium for 2 d. Subsequently, the medium was replaced and the cells were incubated with 0.5 mg ml$^{-1}$ of MTT in complete medium for 4 h. The surviving cells converted MTT to formazan that generates a blue-purple colour when dissolved in dimethylsulfoxide. The intensity was measured at 545 nm using a plate reader (Molecular Dynamics, OPTImax). The relative percentage of survival was calculated by dividing the absorbance of nanoparticle-treated cells by that of the untreated cells.

### 2.5. Apoptotic cell observation

To evaluate whether nanodiamond induced apoptosis, the adherent cells were cultured on a coverslip in a 60 mm Petri dish and then treated with cNDs. Sodium arsenite, a human carcinogen which induces apoptosis in various human cells, was used as a positive control in this study. After treatment with 100 nm cNDs (100 $\mu$g ml$^{-1}$ for 48 h) or sodium arsenite (10 $\mu$M for 48 h), the cells were carefully and slightly washed with isotonic PBS (pH 7.4) and incubated with 4% paraformaldehyde solution in PBS for 1 h at 37 °C. The microtubule of the cytoskeleton was stained with anti-$\beta$-tubulin Cy3 (1:50) for 30 min at 37 °C. Then the nuclei were stained with 2.5 $\mu$g ml$^{-1}$ Hoechst 33258 for 30 min at room temperature. The morphology of apoptosis was confirmed by observation of the nuclear condensation, fragmentation, cell membrane blebbing, cytoskeleton disruption, and formation of apoptotic bodies under phase contrast and fluorescence microscopes.

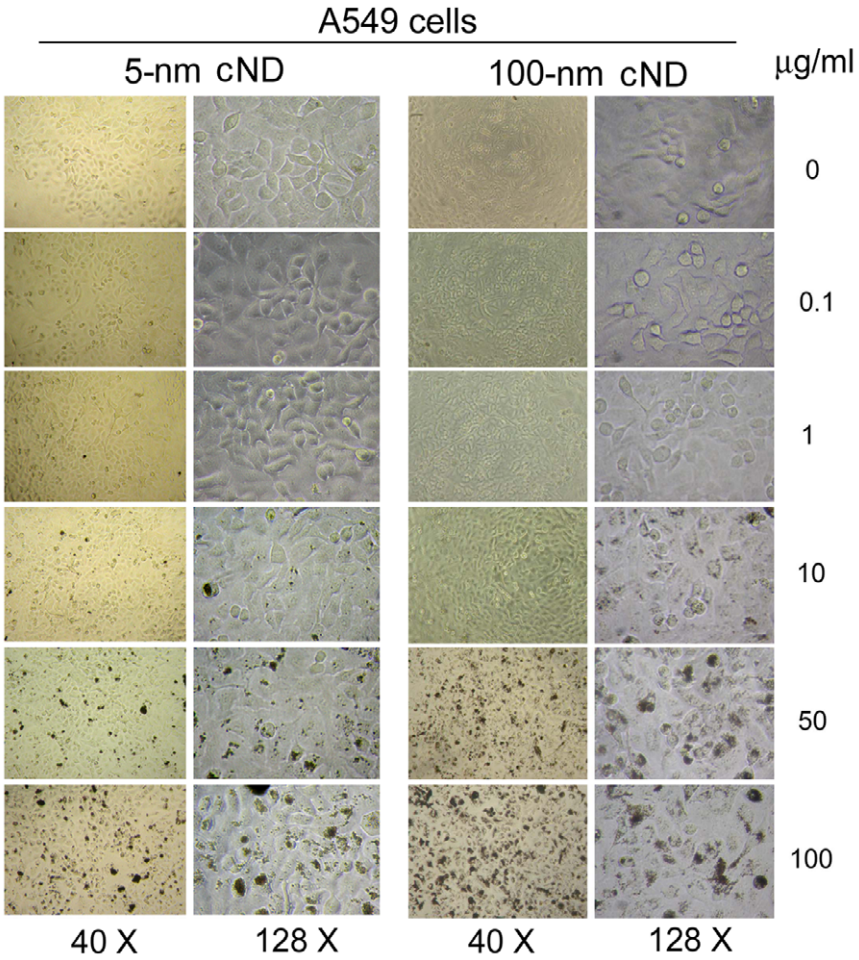


**Figure 1.** Accumulation of 5 and 100 nm cNDs on A549 cells. A549 cells were incubated with or without cNDs for 4 h, and then replaced fresh medium for re-cultured 48 h. The interaction of cNDs and cells was observed under a phase contrast microscope. Black spots indicated cNDs located on cells.

### *2.6. Sodium dodecyl sulfate-polyacrylamide gel (SDS-PAGE) analysis*

To analyse the protein expression profile after treatment with cNDs, the total cell extracts were collected as described [19]. Briefly, cells were lysed in the ice-cold cell extraction buffer (pH 7.6) containing the protease inhibitors (1 $\mu$g ml$^{-1}$ aprotinin, 0.5 $\mu$g ml$^{-1}$ leupeptin and 100 $\mu$g ml$^{-1}$ 4-(2-aminoethyl)benzenesulfonyl fluoride). The cell extracts were gently rotated at 4 °C for 30 min. After centrifugation, the pellets were discarded and supernatant protein concentrations were determined by the BCA protein assay kit (Pierce, Rockford, IL). Equal amounts of proteins (30 $\mu$g/well) were subjected to electrophoresis by 12% SDS-PAGE. After electrophoresis, the gel was stained with the coomassie blue buffer (0.1% coomassie blue, 10% acetic acid and 45% methanol) for 1 h.

### *2.7. Bio-atomic force microscopy (Bio-AFM)*

To measure the size and distribution of cNDs, the 100 nm cND particles (50 $\mu$g ml$^{-1}$) were dropped on a mica slice and were analysed by a bio-atomic force microscope (NanoWizard, JPK Instruments, Berlin). To further examine the interaction of cND and cell, A549 cells were plated at a density of $1 \times 10^5$ on a coverslip, which was kept in a 35 mm Petri dish for 16–20 h before treatment. After treatment with or without 100 $\mu$g ml$^{-1}$ cNDs for 4 h, the cells were washed twice with isotonic PBS (pH 7.4) and fixed in 4% paraformaldehyde solution in PBS for 1 h at 37 °C. Finally, the fixed cells were imaged under Bio-AFM. Bio-AFM was mounted on an inverted microscope, TE-2000-U (Nikon, Japan). The silicon nitride non-sharpened cantilevers used had a nominal force constant of 0.06 N m$^{-1}$ (DNP-20, Veeco). Imaging was performed using contact mode. Line scan rates varied from 0.5 to 2 Hz.

### *2.8. Flow cytometry*

A549 cells were plated at a density of $7 \times 10^5$ cells per 60 mm Petri dish in complete medium for 16–20 h. Thereafter, the cells were treated with 0–100 $\mu$g ml$^{-1}$ cNDs for 4 h. After cND treatment, the cells were washed twice with PBS and were re-cultured in complete medium for 2 days. At the end of incubation, the cells were collected and fixed with ice-cold 70% ethanol overnight at −20 °C. To avoid cell aggregation, the cell solutions were filtered through a nylon membrane (BD

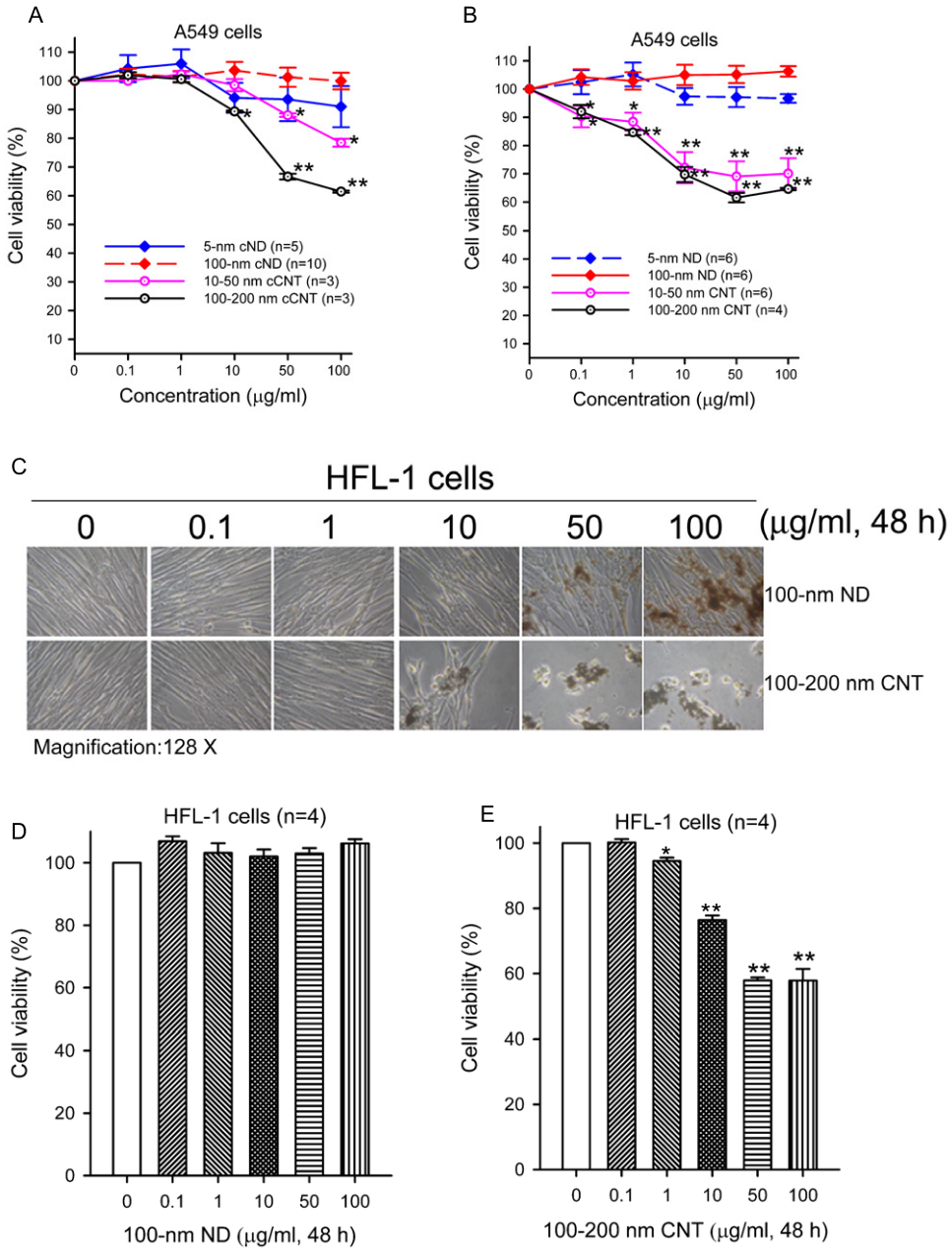


**Figure 2.** Effect of cND, cCNT, ND and CNT on the cytotoxicity in A549 and HFL-1 cells. (A) A549 cells were treated with or without various sizes of cNDs and cCNTs (0.1–100 $\mu$g ml$^{-1}$ for 4 h). (B) A549 cells were treated with or without various sizes of NDs and CNTs (0.1–100 $\mu$g ml$^{-1}$ for 4 h). After treatment, the cells were washed twice with PBS, and were re-cultured in fresh medium for 48 h. The cell viability was measured by MTT assay. The bar represents mean ± S.E. $^{*}p < 0.05$ and $^{**}p < 0.01$ indicate significant difference between untreated and treated samples. (C) The cell population of HFL-1 cells after treatment with or without 100 nm ND and 100–200 nm CNT (100 $\mu$g ml$^{-1}$ for 48 h) was observed under a phase contrast microscope. (D) HFL-1 cells were treated with or without 100 nm NDs (0.1–100 $\mu$g ml$^{-1}$ for 48 h). (E) HFL-1 cells were treated with or without 100–200 nm CNTs (0.1–100 $\mu$g ml$^{-1}$ for 48 h). The cell viability was measured by MTT assay. The bar represents mean ± S.E. $^{*}p < 0.05$ and $^{**}p < 0.01$ indicate significant difference between untreated and treated samples.

Biosciences, San Jose, CA). Subsequently, the samples were analysed by flow cytometer (BD Biosciences). A minimum of ten thousand cells were analysed. The fluorescence from the cNDs was excited at a wavelength 488 nm and the emission was collected in the green light signal range. The fluorescence intensity was quantified by CellQuest software (BD Biosciences).

### *2.9. Confocal microscopy*

The cells were cultured on coverslips, which were kept in a 35 mm Petri dish for 16–20 h before treatment. After treatment with or without cNDs, the cells were washed with isotonic PBS (pH 7.4), and then were fixed with 4% paraformaldehyde solution in PBS for 1 h at 37 °C. Thereafter, the coverslips were

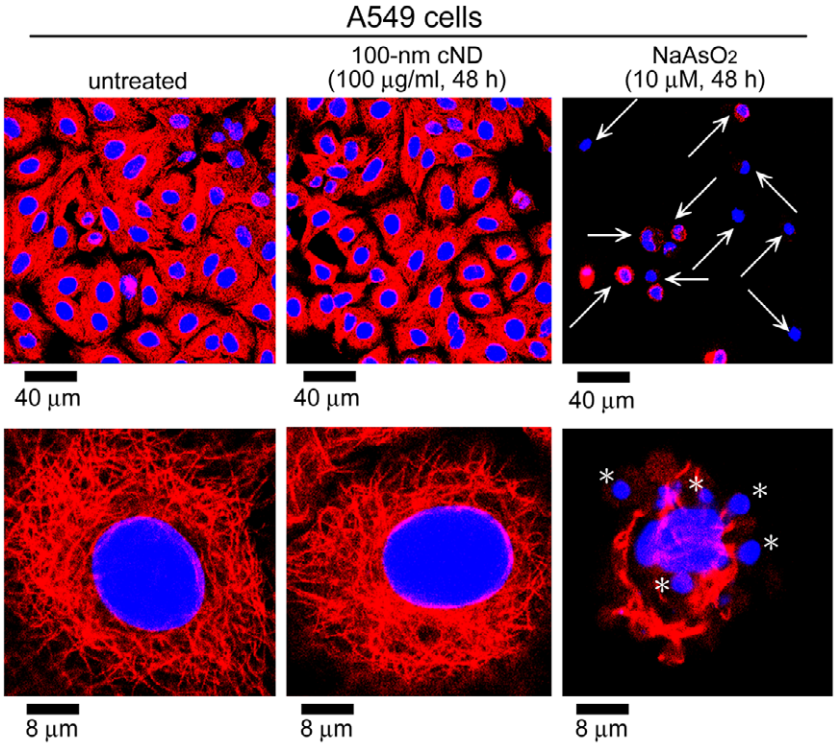


**Figure 3.** Observation of apoptotic cells following treatment with 100 nm cND and sodium arsenite. The adherent cells were cultured on a coverslip in a 60 mm Petri dish and then treated with or without 100 nm cNDs (100 $\mu$g ml$^{-1}$ for 48 h) and sodium arsenite (10 $\mu$M for 48 h). At the end of treatment, the cells were carefully and slightly washed with isotonic PBS, and then fixed with 4% paraformaldehyde solution. The microtubule of the cytoskeleton was stained with anti-$\beta$-tubulin Cy3 that presented with a red colour. The nuclei were stained with Hoechst 33258 that presented with a blue colour. The arrows indicate the morphology of apoptosis, which contained the nuclear condensation and microtubule (cytoskeleton) disruption. The stars represent the apoptotic nuclear fragments and bodies.

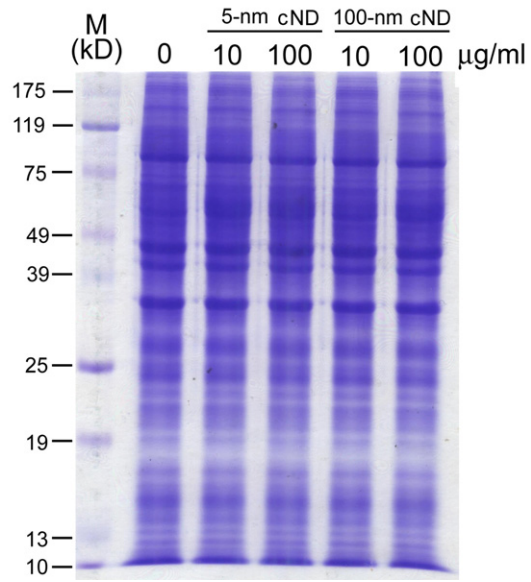


**Figure 4.** Effect of 5 and 100 nm cNDs on the protein expression profile in A549 cells. A549 cells were incubated with or without cNDs for 4 h, and then replaced fresh medium for re-cultured 48 h. At the end of incubation, the total protein extracts were prepared for SDS-PAGE analysis. The left lane indicated the loading marker of proteins.

washed three times with PBS and non-specific binding sites were blocked in PBS containing 10% FBS, 0.3% Triton X-100 for 1 h. The cytoskeleton of $\beta$-tubulin protein was stained with anti-$\beta$-tubulin Cy3 (1:50) for 30 min at 37 °C. Finally, the samples were examined under a Leica confocal laser scanning microscope (Mannheim, Germany) equipped with a UV laser (351/364 nm), an Ar laser (457/488/514 nm) and a HeNe laser (543/633 nm).

### *2.10. Statistical analysis*

Data were analysed using Student's $t$ test, and a $p$ value of $<0.05$ was considered as statistically significant in the experiments.

## 3. Results

### *3.1. Low cytotoxicity and changeless protein expression of cND particles on human lung epithelial cell*

The interaction of cNDs and cells was observed under a phase contrast microscope. A549 cells were incubated with 5 or 100 nm cNDs (0.1–100 $\mu$g ml$^{-1}$ for 4 h) and then replaced fresh medium for re-cultured 48 h. The black spots of cND particles were accumulated on A549 cells via a concentration-dependent manner (figure 1). We found 5 and 100 nm cNDs retained on A549 lung cells after the recovery time (48 h) although cells were treated with cND for only 4 h. To further examine the cytotoxicity after treatment with cNDs, the cND-treated cells were

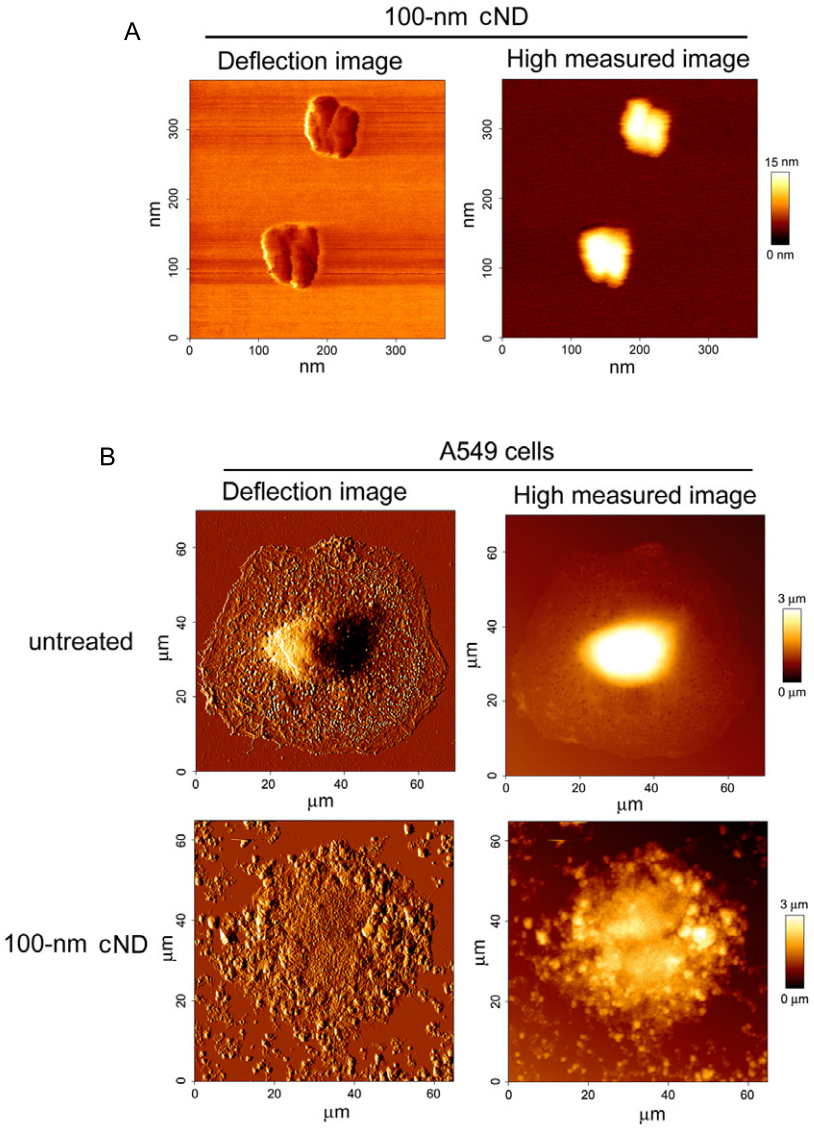


**Figure 5.** Observation of 100 nm cND interacted with cell by Bio-AFM. (A) The 100 nm cND particles were coated on the mica slice and were observed by Bio-AFM. The deflection image of Bio-AFM shows the contour of cNDs, and the 100 nm cND's particles displayed ∼100 nm diameter. (B) A549 cells were treated with or without 50 $\mu$g ml$^{-1}$ 100 nm cNDs for 4 h. After cell fixation, the cells were observed by Bio-AFM. The upper pictures indicated the cND-untreated cell. The lower pictures showed that the cell was treated with 100 nm cND.

subjected to MTT assay. Treatment with 100 nm cNDs (0.1–100 $\mu$g ml$^{-1}$) did not significantly induce cytotoxicity in the A549 lung epithelial cells (figure 2(A)). The size of 5 nm cNDs at 10–100 $\mu$g ml$^{-1}$ slightly reduced cell viability; however, it is not statistically significant. Furthermore, the diameters of 10–50 nm or 100–200 nm of carboxylated carbon nanotubes (cCNTs) significantly decreased cell viability at 10–100 $\mu$g ml$^{-1}$ (figure 2(A)). We have further compared the cytotoxicity of uncarboxylated ND and CNT in A549 cells. Consistently, both 5 and 100 nm NDs did not induce cell death in A549 cells (figure 2(B)), but the CNT particles decreased by approximately 30%–40% cell death at treatment with 10–100 $\mu$g ml$^{-1}$ (figure 2(B)). Besides, we analysed the cell viability in HFL-1 cells after treatment with ND and CNT. The HFL-1 cell population was reduced after treatment with 100–200 nm CNT (100 $\mu$g ml$^{-1}$ for 48 h) under the observation of a phase contrast microscope (figure 2(C), lower pictures). The ND particles were accumulated on HFL-1 cells by 10–100 $\mu$g ml$^{-1}$ for 48 h but did not alter the cell number (figure 2(C), upper pictures). The MTT assays also confirmed that 100 nm ND (0.1–100 $\mu$g ml$^{-1}$ for 48 h) did not reduce the cell viability (figure 2(D)); in contrast, CNT (1–100 $\mu$g ml$^{-1}$ for 48 h) induced cytotoxicity in HFL-1 cells (figure 2(E)).

To examine whether cNDs affect the apoptosis, A549 cells were treated with 100 nm cND (100 $\mu$g ml$^{-1}$ for 48 h) and subjected to cytoskeleton and nuclear staining. The red fluorescence intensity exhibited by microtubule proteins of the cytoskeleton, and the blue colour indicated nuclei by staining with Hoechst 33258 (figure 3). Sodium arsenite, a well-known apoptotic inducer, was used as a positive control in this study. Treatment with sodium arsenite (10 $\mu$M for 48 h) markedly induced the nuclear condensation and cytoskeleton disruption (figure 3, arrows). The formation of apoptotic nuclear fragments and bodies was induced by sodium arsenite

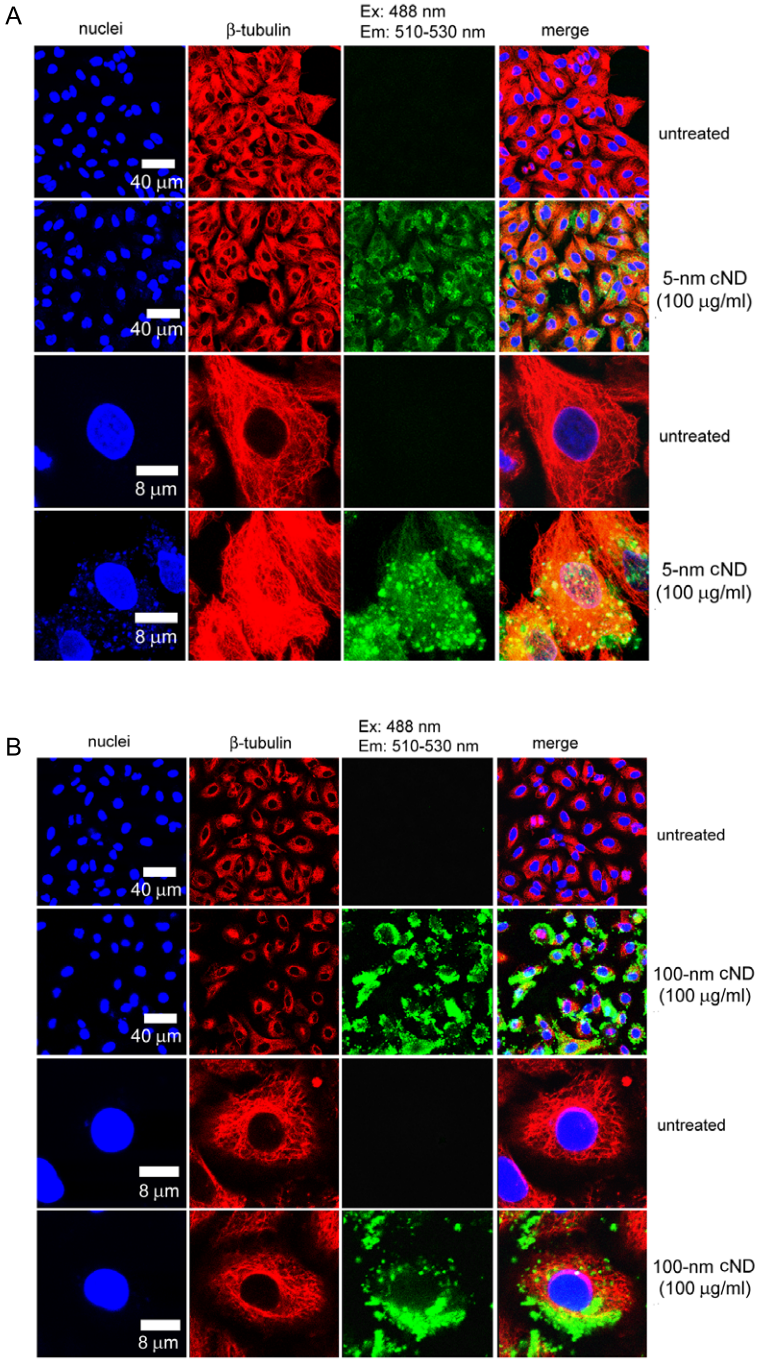


**Figure 6.** Detection of cNDs in A549 cells by a laser scanning confocal microscope. A549 cells were treated with or without 100 $\mu$g ml$^{-1}$ (A) 5 nm cNDs or (B) 100 nm cNDs for 4 h and then recovery for 24 h. After cell fixation, the cells were incubated with the Cy3-labelled anti-$\beta$-tubulin. The green light signal from the cNDs was excited with wavelength 488 nm and the emission was collected in the range of 510–530 nm. The $\beta$-tubulin protein displayed red fluorescence. The nuclei were stained with Hoechst 33258, which displayed blue fluorescence.

(figure 3, stars). Comparing with untreated cells, 100 nm cND (100 $\mu$g ml$^{-1}$ for 48 h) did not alter the morphology of cytoskeleton and nuclei in A549 cells (figure 3, left and middle pictures). Subsequently, the effect of cNDs on the protein expression in A549 cells was analysed by SDS-PAGE assay. The protein expression profile on SDS-PAGE was not markedly altered following treatment with 5 and 100 nm cNDs (figure 4).

### *3.2. Detection of cNDs on human lung epithelial cell by Bio-AFM*

To visualize the interaction of cND and cell, A549 cells were treated with 100 nm cNDs and analysed by Bio-AFM. As shown in figure 5(A), the deflection image of Bio-AFM showed clearly the contour of cNDs with a diameter of ~100 nm. The deflection image of the untreated A549 cell revealed the cell size was ~60 $\mu$m in diameter. The middle

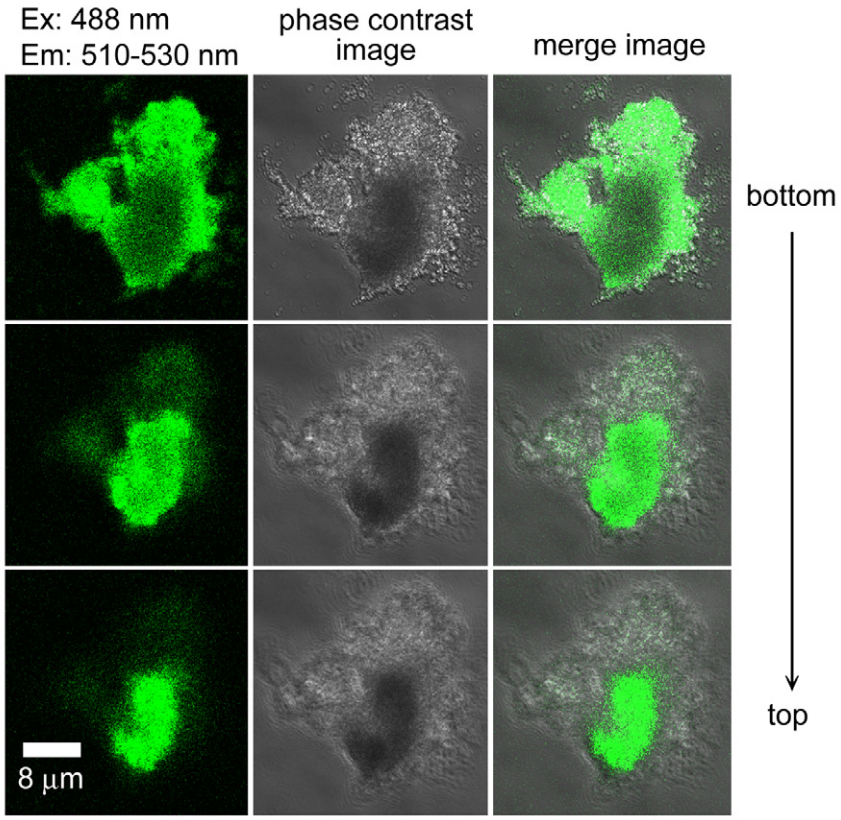


**Figure 7.** *Z*-axis scanning image of cNDs in a living A549 cell by laser scanning confocal microscope. A living A549 cell from treatment with 100 nm cND (100 $\mu$g ml$^{-1}$ for 4 h) was captured in the images by using confocal microscopy. The green light signal from the cNDs was excited with 488 nm wavelength and the emission was collected in the range of 510–530 nm. The distribution of cNDs is inside of the cell when scanning the confocal microscope in vertical direction from bottom to top. The phase contrast images indicate the cell morphology.

protrusion (figure 5(B), upper pictures, left) and the highlight of high measured image (figure 5(B), upper pictures, right) indicated the nuclear location of the cell. The cell was clearly accumulated with cND particles after treatment with 50 $\mu$g ml$^{-1}$ 100 nm cNDs for 4 h (figure 5(B), lower pictures, left). The light spots of high measured image indicated the location of cND particles, which were concentrated on the cell (figure 5(B), lower pictures, right).

### *3.3. Detection of A549 cells with cNDs by laser scanning confocal microscope*

To examine the fluorescence property of cNDs, they were examined under a confocal microscope. The 5 and 100 nm cND particles exhibited green fluorescence on A549 cells at 510–530 nm (emission wavelength) after 488 nm (excitation wavelength) excitation (figures 6(A) and (B)). The cytoskeleton of $\beta$-tubulin protein was stained with the Cy3-labeled mouse anti-$\beta$-tubulin. The red fluorescence (Cy3) exhibited by $\beta$-tubulin that presented the cell morphology of A549 cells (figures 6(A) and (B)). Both 5 and 100 nm cND particles were detected on cells evidenced by the green fluorescence (figures 6(A) and (B)). Furthermore, we have examined the uptake ability of cNDs into cell. The *Z*-axis scanning images of cNDs in A549 cells were analysed by a laser scanning confocal microscope. The cross-section images of a living A549 cell after treatment with 100 nm cND (100 $\mu$g ml$^{-1}$ for 4 h) were captured by confocal microscopy (figure 7). The green fluorescence from the cNDs was excited with 488 nm wavelength and the emission was collected in the range of 510–530 nm. These cNDs particles were ingested inside A549 cells by dissection of the *Z* axis from bottom to top (figure 7).

### *3.4. Detection of A549 cells with cNDs by flow cytometer*

To quantify the fluorescence intensity of cNDs in cells, A549 cells were treated with cNDs and then were analysed by a flow cytometer. Treatment with 5 or 100 nm cNDs on A549 cells elevated the green fluorescence intensity via a concentration-dependent manner (figures 8(A) and (B)). The quantified fluorescence intensity was increased about 4–6 fold after treatment with 5 nm cNDs (50–100 $\mu$g ml$^{-1}$) in A549 cells (figure 8(C)). The 100 nm cND-treated cells were increased 2–3 fold in fluorescence intensity than untreated cells (figure 8(D). The fluorescence intensity of 5 nm cNDs in A549 cells was relatively higher than 100 nm cNDs at equal concentration treatment (figures 8(C) and (D)).

## 4. Discussion

Detectable nanoparticles conjugated with biological molecules are useful for imaging and application [8, 9]. Qdots display

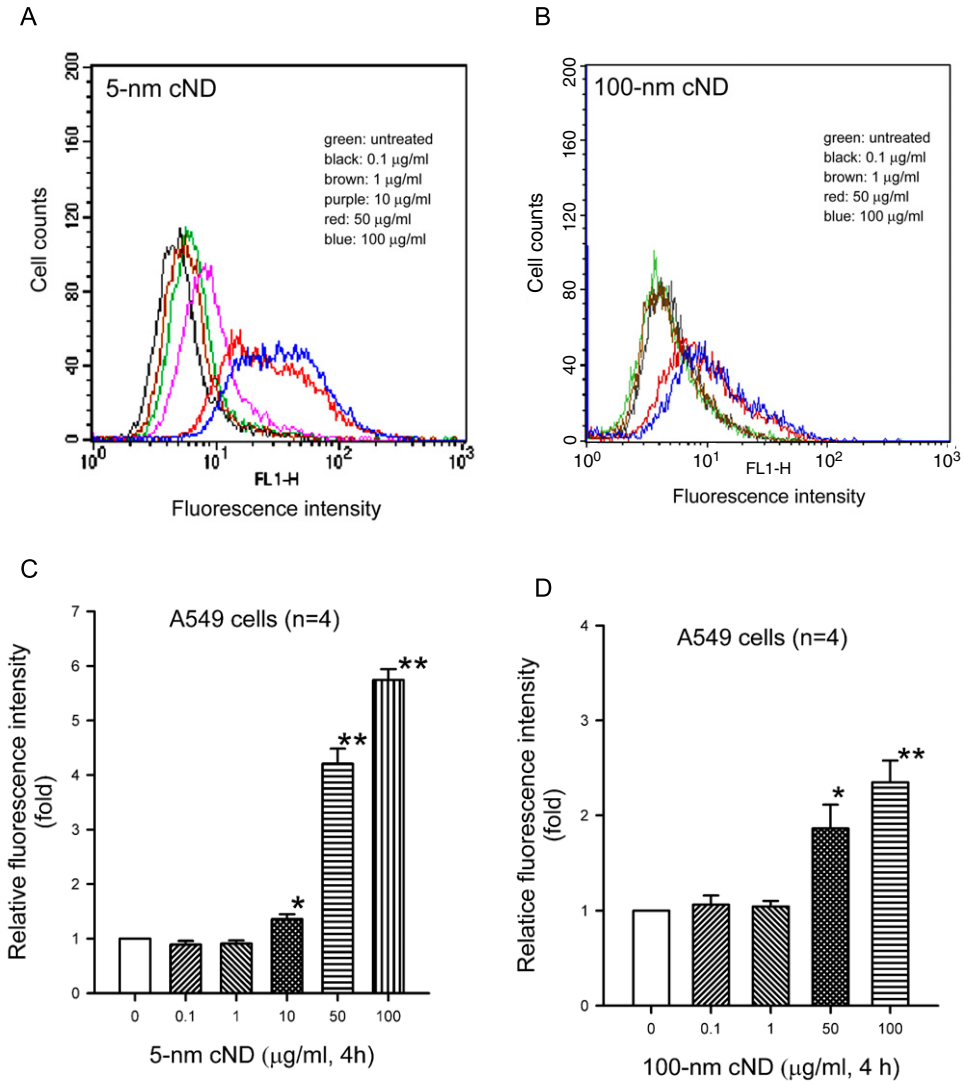


**Figure 8.** Detection of cNDs in A549 cells by flow cytometer. A549 cells were treated with or without (A) 5 nm or (B)100 nm cNDs for 4 h and then recovery for 48 h. At the end of treatment, the cells were trypsinized and then subjected to flow cytometer analysis. (C) and (D), the fluorescence intensities were quantified by a CellQuest software of flow cytometer. The bar represents mean ± S.E. $^{*}p < 0.05$ and $^{**}p < 0.01$ indicate significant difference between untreated and treated samples.

various fluorescence colours that are stable and suitable for labelling and detection [10, 11]. The specific peptide- or antibody-conjugated qdots have been shown to recognize the tumours of mice [8, 13]. Aside from qdots, modification of the nanodiamond's surface by carboxylation has recently been used to conjugate bio-molecules including DNA and protein [3, 5, 6]. For any sensible practice, the toxicity of nanomaterials is a critical problem for biomedical applications. The existence of heavy metals in qdots such as cadmium (a well-known human carcinogen) poses a hazard for medical application. It has been shown that nanotubes display cytotoxicity in alveolar macrophage [17]. We found in this experiment that nanotubes induced cytotoxicity in human lung cells. However, treatment with 5 or 100 nm cNDs did not induce cell death and apoptosis although cND particles were retained on lung cells. Furthermore, cNDs did not alter the protein expression profile in these cells. Recently, it has been reported that the size range from 2 to 10 nm nanodiamonds was not toxic in neuroblastoma cells [20]. Nanodiamonds display little cytotoxicity on human kidney cells [18]. Accordingly, these results suggest that cNDs are biocompatible nanoparticles for further biomedical applications.

We also demonstrated that cNDs are detectable by flow cytometry, confocal microscopy and Bio-AFM. The green fluorescence light emitted in the range from 510 to 530 nm for both 5 and 100 nm cND particles and these light emissions can be detected by flow cytometry and confocal microscopy with 488 nm laser excitation in A549 cells. Indeed, a recent study has proved that nanodiamonds emitted green fluorescence by exciting with higher energy laser, due to the quantum confinement effect [21], unlike the defects of the negatively charged nitrogen–vacancy centre $(N{-}V)^{-}$ which may emit the extended red light [18]. Namely, the green fluorescence may not be from the impurity in the bulk structure of the single-crystal diamond. The mechanism responsible for this green

light emission has been proposed by taking into account the effect of surface states and large surface-to-volume ratio of nanoparticles [21]. This surface quantum effect mechanism may explain the reason that the fluorescence intensity of 5 nm cNDs was relative higher than 100 nm cNDs in these cells at equal concentration treatment, due to the higher surface-to-volume ratio of 5 nm cNDs. Nevertheless, we cannot exclude the possibility that the higher fluorescence intensity observed in 5 nm cNDs than in 100 nm cNDs is because of a higher uptake ability for the smaller cND sizes. Furthermore, the observed fluorescence was from the ND or cND that were not subjected to high-energy electron or proton treatments, i.e. the natural defects/impurities may provide fluorescence intensity strong enough for confocal microscopy or flow cytometry detection. The cNDs particles have been shown to exhibit high affinity for proteins through both hydrophilic and hydrophobic force interaction [4]. Therefore, the cND's fluorescence is suitable for further bio-applications (imaging and detection) after conjugation with specific bio-molecules.

We have examined the uptake ability of cNDs into cells by the $Z$-axis scanning images of cNDs in A549 cells under laser confocal microscope analysis. We clearly found that cNDs were located in the cytoplasma of lung cells. Both 5 and 100 nm cNDs were taken up into cells. The images of Bio-AFM also showed the lung cell accumulated cND particles. Importantly, we can quantify the fluorescence intensities of cNDs in the cells by flow cytometry. 5 or 100 nm cND particles elevated the green fluorescence via a concentration-dependent manner in lung cells. These data indicate that cNDs can be taken into the cells. It has been shown that carbon particles can be taken into cells by endocytosis [22]. Thus, we suggest that cNDs may interact with the proteins of the cell membrane for the uptake and accumulation in human lung cells; nevertheless, the existence of cNDs inside a cell does not induce cytotoxicity.

In conclusion, we have shown that cNDs can be easily detected by bio-AFM, confocal microscopy and flow cytometry. The biocompatible and detectable properties of cNDs are suitable for further biomedical applications including bio-labelling, imaging and drug delivery.

## Acknowledgments

This work was supported by grants from NSC 94-2120-M-259-002 and NSC 94-2120-M-259-003.

## References

[1] Poh W C, Loh K P, De Zhang W, Triparthy S, Ye J S and Sheu F S 2004 Biosensing properties of diamond and carbon nanotubes *Langmuir* **20** 5484–92
[2] Carlisle J A 2004 Precious biosensors *Nat. Mater.* **3** 668–9
[3] Yang W *et al* 2002 DNA-modified nanocrystalline diamond thin-films as stable, biologically active substrates *Nat. Mater.* **1** 253–7
[4] Kong X L, Huang L C, Hsu C M, Chen W H, Han C C and Chang H C 2005 High-affinity capture of proteins by diamond nanoparticles for mass spectrometric analysis *Anal. Chem.* **77** 259–65
[5] Ushizawa K, Sato Y, Mitsumori T, Machinami T, Ueda T and Ando T 2002 Covalent immobilization of DNA on diamond and its verification by diffuse reflectance infrared spectroscopy *Chem. Phys. Lett.* **351** 105–8
[6] Huang L C and Chang H C 2004 Adsorption and immobilization of cytochrome c on nanodiamonds *Langmuir* **20** 5879–84
[7] Kossovsky N, Gelman A, Hnatyszyn H J, Rajguru S, Garrell R L, Torbati S, Freitas S S and Chow G M 1995 Surface-modified diamond nanoparticles as antigen delivery vehicles *Bioconjug. Chem.* **6** 507–11
[8] Akerman M E, Chan W C, Laakkonen P, Bhatia S N and Ruoslahti E 2002 Nanocrystal targeting *in vivo Proc. Natl Acad. Sci. USA* **99** 12617–21
[9] Alivisatos P 2004 The use of nanocrystals in biological detection *Nat. Biotechnol.* **22** 47–52
[10] Dahan M, Levi S, Luccardini C, Rostaing P, Riveau B and Triller A 2003 Diffusion dynamics of glycine receptors revealed by single-quantum dot tracking *Science* **302** 442–5
[11] Michalet X, Pinaud F F, Bentolila L A, Tsay J M, Doose S, Li J J, Sundaresan G, Wu A M, Gambhir S S and Weiss S 2005 Quantum dots for live cells, *in vivo* imaging, and diagnostics *Science* **307** 538–44
[12] Souza G R, Christianson D R, Staquicini F I, Ozawa M G, Snyder E Y, Sidman R L, Miller J H, Arap W and Pasqualini R 2006 Networks of gold nanoparticles and bacteriophage as biological sensors and cell-targeting agents *Proc. Natl Acad. Sci. USA* **103** 1215–20
[13] Gao X, Cui Y, Levenson R M, Chung L W and Nie S 2004 *In vivo* cancer targeting and imaging with semiconductor quantum dots *Nat. Biotechnol.* **22** 969–76
[14] Colvin V L 2003 The potential environmental impact of engineered nanomaterials *Nat. Biotechnol.* **21** 1166–70
[15] Oberdorster G *et al* 2005 Principles for characterizing the potential human health effects from exposure to nanomaterials: elements of a screening strategy *Part Fibre. Toxicol.* **2** 8
[16] Hoet P H, Bruske-Hohlfeld I and Salata O V 2004 Nanoparticles—known and unknown health risks *J. Nanobiotechnol.* **2** 12
[17] Jia G, Wang H, Yan L, Wang X, Pei R, Yan T, Zhao Y and Guo X 2005 Cytotoxicity of carbon nanomaterials: single-wall nanotube, multi-wall nanotube, and fullerene *Environ. Sci. Technol.* **39** 1378–83
[18] Yu S J, Kang M W, Chang H C, Chen K M and Yu Y C 2005 Bright fluorescent nanodiamonds: no photobleaching and low cytotoxicity *J. Am. Chem. Soc.* **127** 17604–5
[19] Chao J I, Kuo P C and Hsu T S 2004 Down-regulation of survivin in nitric oxide-induced cell growth inhibition and apoptosis of the human lung carcinoma cells *J. Biol. Chem.* **279** 20267–76
[20] Schrand A M, Huang H, Carlson C, Schlager J J, Omacr Sawa E, Hussain S M and Dai L 2007 Are diamond nanoparticles cytotoxic? *J. Phys. Chem.* B **111** 2–7
[21] Zhao F L, Gong Z, Liang S D, Xu N S, Deng S Z, Chen J and Wang H Z 2004 Ultrafast optical emission of nanodiamond induced by laser excitation *Appl. Phys. Lett.* **85** 914–6
[22] Kam N W S, Liu Z and Dai H 2006 Carbon nanotubes as intracellular transporters for proteins and DNA: an investigation of the uptake mechanism and pathway *Angew. Chem. Int. Edn* **45** 577–81